

# A mean field model for brownian and turbulent coagulation of polydispersed aerosols

A.T. Celada and A. Salcido

*Instituto de Investigaciones Eléctricas,  
Gerencia de Sistemas de Calidad, Ambiente y Seguridad,  
Reforma No. 113, Col. Palmira, 62490 Cuernavaca, Morelos, México,  
e-mail: atcelada@iie.org.mx*

Recibido el 3 de noviembre de 2004; aceptado el 19 de abril de 2005

A mean field model for Brownian and turbulent coagulation of polydispersed aerosols is proposed. This model is based on a discrete balance equation that gives the rate of change for the number density of particles with diameters within a given range in terms of the rates of formation and loss of particles in all other diameter ranges. A monomer structure for the particles is not considered in this model, differing in this sense from the Smoluchowsky theory. Instead, it uses a probabilistic estimate of formation or loss of particles which depends on the diameters ranges of the colliding particles. To test this model, five aerosol coagulation experiments, carried out by Kim *et al.* [1], Rooker and Davies [2], and Okuyama *et al.* [3] were used to try to reproduce the results. The computer simulation results were found in good agreement with the experimental data.

**Keywords:** Polydispersed aerosols; brownian coagulation; turbulent coagulation; mathematical modelling.

En este trabajo se propone un modelo de campo medio para describir el proceso de la coagulación browniana turbulenta de los aerosoles polidispersos. Este modelo considera una ecuación de balance discreta que proporciona la rapidez de cambio de la densidad de número de partículas con diámetros en un intervalo de tamaños del aerosol. A diferencia de la teoría de Smoluchowski, en este modelo no se considera la estructura monomérica de las partículas y se realiza una estimación probabilística de formación y pérdida de partículas dependiente de los intervalos de diámetros de las partículas incidentes. Para evaluar el desempeño de éste modelo se realizaron simulaciones tratando de reproducir los resultados de tres series de experimentos de coagulación realizados por Kim *et al.* [1], Rooker y Davies [2], y Okuyama *et al.* [3]. Los resultados obtenidos coinciden satisfactoriamente con los datos experimentales.

**Descriptores:** Aerosoles polidispersos; coagulación browniana; coagulación turbulenta; modelación matemática.

PACS: 82.70.Rr; 92.20.Bk; 92.20.Mt.

## 1. Introduction

Coagulation is an important process of growing and the size distribution of fine particles (with diameters ranging from 0.01 to 1.00  $\mu\text{m}$ ) in aerosols. Air pollution models, which take into account the transport and dispersion phenomena of atmospheric aerosols, must include the coagulation process for the proper assessment of their impacts on air quality. Also in engineering areas where the processes depend on the particle size distribution (*e.g.* painting, residual water treatment, etc.) the aerosol coagulation is a relevant phenomenon. As a result of the fossil fuel combustion in industry, a wide variety of fine and large particles are produced and emitted to the atmosphere together with the residual gases of combustion. The initial size distribution of these aerosol particles changes during the first minutes after emission due to a growing process such as that of coagulation [4,5]. In general, the main mechanisms that allow the coagulation of the atmospheric aerosol are the brownian motion and turbulence [6,7,8,9]. Although both mechanisms act simultaneously, while the movement of the big particles is controlled by the mean wind and atmospheric turbulence, the movement of fine particles is related mainly to the brownian motion. Under atmospheric conditions with high turbulence intensity, turbulent coagulation will dominate the coagulation process of both large and fine particles [6,7].

The first theoretical description of the coagulation phenomenon was proposed by Smoluchowsky in 1917 [4,5]. He considered the problem of finding the time evolution of the particle size distribution of spherical particles in aerosols, all of them with the same diameter, initially. Within the Smoluchowsky's theoretical framework, at any time, each aerosol particle could be formed by an integer number of base particles (or monomers), which would be the smallest, simple and stable particles in the aerosol, and the density of the number of particles with  $k$  monomers,  $n_k$ , as a function of time, would be the solution of the following balance equation:

$$\frac{dn_k}{dt} = \frac{1}{2} \sum_{i+j=k} K_{ij}n_i n_j - \sum_{i=1}^{\infty} K_{ik}n_i n_k \quad (1)$$

where  $K_{ij}$  is a coagulation kernel describing the mechanism the mechanism which allows particles to collide each other [4]. The first term at the right hand side of Eq. (1) is the production of the particles with  $k$  monomers due to collisions of particles with  $i$  and  $j$  monomers such that  $i + j = k$ , and the second term is the consumption of particles with  $k$  monomers due to collisions with other aerosol particles. The main assumptions behind the Smoluchowsky theory are as follows: only binary collisions are considered, the collisions conserve the mass and volume, and the aerosol particles coagulate each time they collide.

The Smoluchowsky's theory is the basis for numerous applications both theoretical and experimental [4,5,10,11], however, its application is restricted to monodispersed aerosols. It has been observed that Smoluchowsky's theory fails in predicting the size distribution of the aerosol particles when they are polydispersed, that is, when the aerosol particles are not considered to be made of monomers. In practice, it is not always possible (or easy) identify aerosol's monomers [10], so this forces one to describe the aerosol size distribution in terms of size ranges (or bins).

In this work, we propose a mean field model for the coagulation process (brownian and turbulent) of polydispersed aerosols. As in the Smoluchowsky's theory, we assumed that the aerosol is constituted of spherical particles which coagulate each time they collide. Also, only binary collisions are considered, and mass and volume are assumed to be conserved by collisions. However, the size distribution of the aerosol particles will be described, not in terms of the density of the number of the particles made by a given number of monomers, but in terms of the density of the number of aerosol particles whose diameters range within a given diameter interval. Furthermore, the production (and consumption) of aerosol particles let us thought that they are also regulated by the probability that one collision produces a new particle where diameter ranges within some given diameter interval. This mean field coagulation model (hereafter referred as MFC model) has been tested under both brownian and turbulent conditions in some experiments already reported in literature, such as those of Rooker and Davies [2] and Kim *et al.* [1] for brownian coagulation, and those of Okuyama *et al.* [3] for turbulent brownian coagulation. The simulation results were found in a very good agreement with the experimental ones.

## 2. The mean field coagulation model

Our system a polydisperse aerosol constituted by spherical particles whose diameters range within a diameter interval  $B$ . The whole diameter spectrum  $B$  is divided into a given number  $M$  of subintervals (not necessarily all with the same length), which we will denote by  $\beta_i, i = 1, 2, \dots, M$ . The set of partial spectra  $\beta_i$  is assumed to be a partition of  $B, i.e.$

$$B = \bigcup_{i=1}^M \beta_i, \quad \beta_i \cap \beta_j = \phi \quad i \neq j$$

The concentration of aerosol particles will be described by the variables  $n_k (k = 1, 2, \dots, M)$ , which denote the density of the number of aerosol particles with diameters ranging in  $\beta_k$ . Coagulation of the aerosol particles is assumed to be driven only by binary collisions which preserve mass and volume. When a collision takes place in the system, involving one particle of  $\beta_i$  and another of  $\beta_j$ , the colliding particles will coagulate to produce a new particle which may belong to  $\beta_i$  or  $\beta_j$ , or some other interval  $\beta_k$  depending on the volume of the particle created, which must be equal to the sum of the volumes of the colliding particles. This means that

the production (or consumption) of the aerosol particles in a given  $\beta_k$  can be considered as a function of three factors: the probability  $f$  when one collision takes place in the system, which is determined by the particular mechanism promoting collisions (brownian motion, turbulence, or some others); the probability  $p_{ij}$  when such a collision involves particles of two particular intervals  $\beta_i$  and  $\beta_j$ ; and the probability  $Q_{ij}^k$  when such a collision produce a particle in a given interval  $\beta_k$ . The first two factors may be expressed by just one probability  $P_{ij}$  given by

$$P_{ij} = K(r_i, D_i, r_j, D_j, \dots) \begin{cases} n_i n_j & \text{if } i = j \\ 2n_i n_j & \text{if } i \neq j \end{cases}, \quad (2)$$

where the variables  $n_i$  and  $n_j$  denote the densities of the number of aerosol particles in  $\beta_i$  and  $\beta_j$ , respectively, and  $K$  is a proper coagulation kernel determined by the particular mechanisms which produce the collisions. The kernel  $K$ , of course, will be a function of the properties of the colliding particles, such as the radii  $r_i$  and  $r_j$ , and the brownian diffusion coefficients  $D_i$  and  $D_j$ , and some other properties associated with the motion regime of the gas where the particles are suspended, such as the turbulence parameters.

Now, the rate of change in the density of the number of aerosol particles with diameters ranging in  $\beta_k$  can be expressed by the following balance equation:

$$\frac{dn_k}{dt} = \frac{1}{2} \sum_{i,j \neq k}^M P_{ij} Q_{ij}^k - \sum_{i=1}^M P_{ik} (1 - Q_{ik}^k), \quad (3)$$

where the first term in the right hand side represents the creation of particles in  $\beta_k$  due to collisions of particles of  $\beta_i$  and  $\beta_j$ , and the second term represents the consumption of these particles by their collisions with particles belonging to other subintervals. In this balance equation, we did not include terms to represent the effects of a loss of particles by mechanisms such as wall adherence or others.

The probability factor  $Q_{ij}^k$  takes into account the polydisperse nature of the aerosol, which is related to the volume conservation in the collisions. Although, it may be possible to determine this probability experimentally [12], however, for the purposes of this work we estimated it numerically as follows: for each triplet  $(\beta_i, \beta_j, \beta_k)$ , we considered particle radii,  $r_i$  and  $r_j$ , running with very small steps along the intervals  $\beta_i$  and  $\beta_j$ , respectively, and the respective particle volumes,  $V_i$  and  $V_j$ , were calculated in each case. Furthermore, since volume is assumed to be conserved by coagulation, the volume of the new particle is  $V = V_i + V_j$ . Then, each time  $V$  was consistent with the radius of a particle in  $\beta_k$ , a counter  $q_{ij}^k$  was increased by 1. Finally, the probability  $Q_{ij}^k$  was estimated by dividing the counter  $q_{ij}^k$  by the total number of cases.

In the computer implementation of the MFC model, the probability factor  $Q_{ij}^k$  was introduced by means of a lookup table. In Fig. 1, an schematic illustration of the values of  $Q_{ij}^k$  for different inputs is presented.

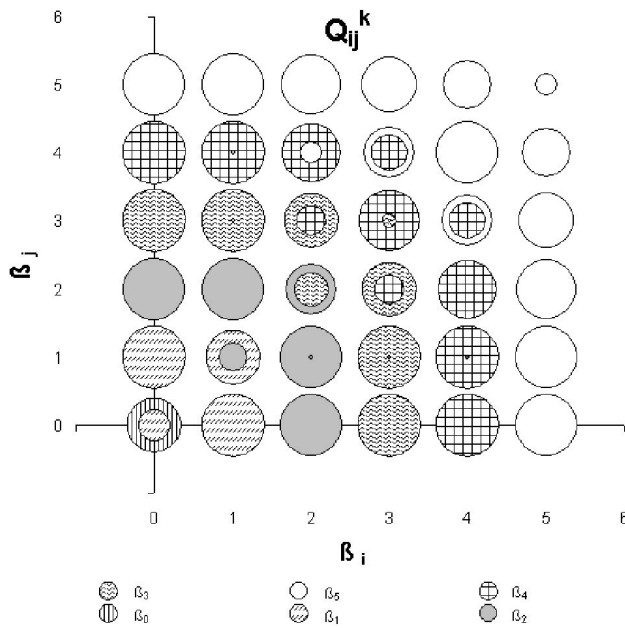


FIGURE 1. Schematic illustration of the values of  $Q_{ij}^k$ .

Inclusion of the probability  $Q_{ij}^k$  to consider the polydispersed nature of the aerosol explicitly makes one of the main differences of the MFC model with other coagulation models [4,5,11,13]. In general, in fact, only few coagulation models include this aerosol characteristic in its expressions. For example, in the model developed by Jacobson in 1994 [14,15,16,17], he proposed a numerical semi-implicit scheme to solve the monomer Smoluchowsky's equation, and introduced a volume fraction  $f_{ijk}$  to distribute the volume of the particle formed by coagulation between adjacent size-bins ( $k$  and  $k+1$ ) when the coagulated particle results with a volume between the volumes of the particles in these bins. This fraction indicates what part of the volume of the new particle will be assigned to bin  $k$  and what part will be assigned to bin  $k + 1$ .

Although the factors  $f_{ijk}$  and  $Q_{ij}^k$  play similar roles in the respective models, in the sense that both of them have introduced to take into account the aerosol's polydispersed nature, there are important differences between them. In the Jacobson's model,  $f_{ijk}$  represents a volume splitting-criterion which distributes the volume of the coagulated particle between adjacent size-bins, but in the MFC model,  $Q_{ij}^k$  is just the probability of creating a particle in the bin  $\beta_k$  as a result of the collision of particles of the bins  $\beta_i$  and  $\beta_j$ . Furthermore, while in the MFC model the size of the bins is arbitrary, in the Jacobson's model, the size of one bin is proportional to the preceding bin, with a constant volume ratio.

Application of Eq. (3) to study the coagulation process requires the knowledge of the coagulation kernel  $K$ , which describes the mechanism by which the aerosol particles are driven to collide. For brownian coagulation of particles suspended in a gas under otherwise equilibrium conditions, we have considered the well known kernel [4, 10, 18] given by

$$K_B = 4\pi(r_i + r_j)(D_i + D_j). \tag{4}$$

Here, however, we interpreted the particle radii  $r_i$  and  $r_j$  as their respective mean-values in  $\beta_i$  and  $\beta_j$ , and the diffusion coefficients  $D_i$  and  $D_j$  as those ones which are consistent with such mean radii Eq. (5):

$$D_i = \frac{\kappa T C_c}{3\pi\mu dp_i} \tag{5}$$

where

$$C_c = 1 + \frac{2\lambda}{dp_i} \left[ 1.257 + 0.4 \exp\left(\frac{-1.1 dp_i}{2\lambda}\right) \right] \tag{6}$$

is the Cunningham slip correction factor, and  $\kappa$  is the Boltzmann constant,  $T$  is the absolute temperature,  $\mu$  is the air viscosity,  $dp_i$  is the mean diameter of particles in the  $\beta_i$  interval, and  $\lambda$  is the mean free path of air molecules.

For brownian coagulation under turbulent conditions, the coagulation kernel is considered, in general, as a superposition of the brownian kernel,  $K_B$ , and some other kernel  $K_T$  which represents the effect of turbulence on the coagulation process.

$$K_{BT} = K_B + K_T \tag{7}$$

In literature, one can find several expressions for  $K_T$  [19,20,21]. In this work we have used the turbulent kernel derived by Kruijs and Kuster [21]:

$$K_T = \varepsilon_c \left(\frac{8\pi}{3}\right)^{1/2} (r_i + r_j)^2 (w_a^2 + w_c^2)^{1/2} \tag{8}$$

where  $\varepsilon_c$  is an empirical coefficient (with values ranging from 1 to 3.5) that we introduced to modulate the collision efficiency, the radii  $r_i$  and  $r_j$ , as above, are interpreted as the mean radii in  $\beta_i$  and  $\beta_j$ , and  $w_a$  and  $w_c$  are the relative particle velocities related to inertial and shear turbulent effects. The expressions defining these last two parameters are described in Table I.

### 3. Results

In order to test the MFC model, we carried out computer simulations for three series of coagulation experiments we found in literature. The coagulation experiments of two of these series were performed for brownian coagulation under no turbulent conditions (experiments of Kim *et al.* [1], and Rooker & Davies [2]). The experiments in the other one were performed under conditions of low and medium turbulence intensity (experiments of Okuyama *et al.* [3]).

### 4. Brownian coagulation

For the case of pure brownian coagulation we used the experimental data obtained by Kim *et al.* [1] (where a NaCl aerosol was considered) and from Rooker & Davies [2] (with a CaCO<sub>3</sub> aerosol). A general description of the experimental

TABLE I. Turbulent Coagulation Kernel by Kruis and Kusters (1997)

$$\beta(v_i, v_j) = \left(\frac{8\pi}{3}\right)^{1/2} (r_i + r_j)^2 (w_a^2 + w_c^2)^{1/2}$$

$$w_a^2 = 3(1 - b)^2 v_f^2 \frac{\gamma}{\gamma - 1} X \left( \frac{(\theta_i + \theta_j)^2 - 4\theta_i \theta_j \sqrt{\frac{1 + \theta_i + \theta_j}{(1 + \theta_i)(1 + \theta_j)}}}{(\theta_i + \theta_j)} \right) X \left[ \frac{1}{(1 + \theta_i)(1 + \theta_j)} - \frac{1}{(1 + \gamma\theta_i)(1 + \gamma\theta_j)} \right]$$

$$w_c^2 = 0.238 b v_f^2 \left( \frac{v_i^2}{v_f^2} \frac{\theta_j}{C_{c_j}} + \frac{v_j^2}{v_f^2} \frac{\theta_i}{C_{c_i}} + 2 \frac{v_i v_j}{v_f^2} \sqrt{\frac{\theta_i \theta_j}{C_{c_i} C_{c_j}}} \right)$$

$$v_f^2 = \frac{\gamma(\varepsilon\nu)^{1/2}}{0.183} \quad b = \frac{3\rho_f}{2\rho_p + \rho_f}$$

$$\theta_i = \frac{\tau_i}{T_L} \quad \theta_j = \frac{\tau_j}{T_L}$$

$$T_L = \frac{0.4v_f^2}{\varepsilon}$$

$$\frac{v_i^2}{v_f^2} = \frac{\gamma}{\gamma - 1} \left( \frac{1 + b^2\theta_i}{1 + \theta_i} - \frac{1 + b^2\gamma\theta_i}{\gamma(1 + \theta_i)} \right) \quad \frac{v_j^2}{v_f^2} = \frac{\gamma}{\gamma - 1} \left( \frac{1 + b^2\theta_j}{1 + \theta_j} - \frac{1 + b^2\gamma\theta_j}{\gamma(1 + \theta_j)} \right)$$

$$\frac{v_i v_j}{v_f^2} = \frac{\gamma}{\gamma - 1} \left( \frac{(\theta_i + \theta_j + 2\theta_i\theta_j) + b(\theta_i^2 + \theta_j^2 - 2\theta_i\theta_j) + b^2(\theta_i^2\theta_j + \theta_i\theta_j^2 + 2\theta_i\theta_j)}{(\theta_i + \theta_j)(1 + \theta_i)(1 + \theta_j)} - \frac{(\theta_i + \theta_j + 2\gamma\theta_i\theta_j) + b\gamma(\theta_i^2 + \theta_j^2 - 2\theta_i\theta_j)}{\gamma(\theta_i + \theta_j)(1 + \gamma\theta_i)(1 + \gamma\theta_j)} + \frac{b^2(\gamma^2\theta_i^2\theta_j + \gamma^2\theta_i\theta_j^2 + 2\gamma\theta_i\theta_j)}{\gamma(\theta_i + \theta_j)(1 + \gamma\theta_i)(1 + \gamma\theta_j)} \right)$$

Where:

- $\beta(v_i, v_j)$  original Kruis and Kuster turbulent kernel
- $r_i, r_j$  radii of the particles as calculated from their volumes:  $r_i = (3v_i/4\pi)^{1/3}$
- $\rho_f$  fluid density
- $\rho_p$  particle density
- $w_a$  relative particle velocity due to inertial turbulent effects
- $w_c$  relative particle velocity due to shear turbulent effects
- $\varepsilon$  kinetic energy dissipation rate per mass unit
- $\nu$  kinematic viscosity of fluid
- $\mu$  dynamic viscosity of fluid
- $v_f$  rms fluid velocity
- $v_i, v_j$  rms particles velocities
- $\gamma$  spectrum constant ranging from 10 to 100
- $b$  added mass coefficient
- $\theta_i$  dimensionless particle relaxation time
- $T_L$  Lagrangian time scale
- $\tau_i, \tau_j$  relaxation times of particles  $\tau_i = \frac{C_{c,i}(2\rho_p + \rho_f)r_i^2}{9\mu}$
- $C_{c,i}$  Cunningham slip correction factor

conditions is presented in Table II. In both cases, the experimental procedure was oriented to evaluate the density of the total number of aerosol particles  $n$  as a function of time, and also for calculating the coefficients of coagulation and wall adherence from the experimental data by using the following equation:

$$\frac{dN}{dt} = -KN^2 + LN \tag{9}$$

In this equation, the first term in the right hand side represents the lost of particles by coagulation, and the second one represents the lost of particles by adherence in walls in the experimental setup. Here,  $K$  and  $L$  denote, respectively, the coefficients of coagulation and wall adherence which were determined experimentally.

TABLE II. General characteristics of the coagulation experiments carried out by Kim *et al.* (2003) and Rooker & Davies (1979).

| <b>Kim <i>et al.</i> (2003)</b>               |   |                          |                       |                         |
|---|---|--------------------------|-----------------------|-------------------------|
| <b>Experimental conditions:</b>               | Mean geometric diameter ( $\mu\text{m}$ ) | No ( $\#/ \text{cm}^3$ ) | L                     | Experiment duration (s) |
| • NaCl Aerosol (initially monodispersed)      |   |                          |                       |                         |
| • Constant temperature and pressure           | 0.050                                     | 1,230,000                | $9.21 \times 10^{-4}$ | 3226                    |
| • Diameters: 0.050 and 0.115 $\mu\text{m}$    | 0.115                                     | 1,150,000                | $2.00 \times 10^{-5}$ | 1800                    |
| • Duration: 1800 – 3226 s                     |   |                          |                       |                         |
| <b>Rooker and Davies (1979)</b>               |   |                          |                       |                         |
| <b>Experimental conditions:</b>               | Experiment ID                             | No ( $\#/ \text{cm}^3$ ) | L                     | Experiment duration (s) |
| • CaCO <sub>3</sub> Aerosol                   |   |                          |                       |                         |
| • Constant temperature and pressure           | C50                                       | 12,060                   | $1.89 \times 10^{-4}$ | 1800                    |
| • Diameter range: 0.005 - 0.030 $\mu\text{m}$ | C63                                       | 15,150                   | $1.52 \times 10^{-4}$ | 1800                    |
| • Duration: 1800 s                            | C90                                       | 254,440                  | $1.89 \times 10^{-4}$ | 1800                    |

TABLE III. Diameter intervals  $\beta_k$  used in the MFC model in the computer simulations of the coagulation experiments by Kim *et al.* and Rooker & Davies.

| <b>Experiments of Kim <i>et al.</i></b>    |                                  |  |                                  | <b>Experiments of Rooker &amp; Davies</b> |                                  |
|--|----------------------------------|--|----------------------------------|---|----------------------------------|
| <b>Exp. 0.050 <math>\mu\text{m}</math></b> |                                  | <b>Exp. 0.115 <math>\mu\text{m}</math></b> |                                  |   |                                  |
| Interval                                   | Diameter Range ( $\mu\text{m}$ ) | Interval                                   | Diameter Range ( $\mu\text{m}$ ) | Interval                                  | Diameter Range ( $\mu\text{m}$ ) |
| 1  | 0.010 to 0.090                   | 1  | 0.025 to 0.050                   | 1   | 0.005 to 0.010                   |
| 2  | 0.090 to 0.180                   | 2  | 0.050 to 0.060                   | 2   | 0.010 to 0.015                   |
| 3  | 0.180 to 0.360                   | 3  | 0.060 to 0.080                   | 3   | 0.015 to 0.020                   |
|  |                                  | 4  | 0.080 to 0.100                   | 4   | 0.020 to 0.025                   |
|  |                                  | 5  | 0.100 to 0.130                   | 5   | 0.025 to 0.030                   |
|  |                                  | 6  | 0.130 to 0.260                   | 6   | 0.030 to 0.100                   |
|  |                                  | 7  | 0.260 to 0.520                   |   |                                  |
|  |                                  | 8  | 0.520 to 0.800                   |   |                                  |
|  |                                  | 9  | 0.800 to 1.600                   |   |                                  |
|  |                                  | 10   | 1.600 to 4.000                   |   |                                  |

In the computer simulations that we carried out with the MFC model, the diameter range was divided in three and ten subintervals in the case of the experiments of Kim *et al.* [1], and in six diameter subintervals in the case of the experiments of Rooker & Davies [2], such as described in Table III. The density of the number of particles in each subinterval was numerically evaluated during 1800 and 3226 s in the first case, and during 1800 s in the second one, with time steps of 1s in all cases. For comparison purposes, the density of the total number of particles was calculated, each time-step, from the densities in the subintervals considered, and it was corrected to take into account the wall adherence effect by using the wall adherence coefficient,  $L$ , provided by the authors of each experiment (see Table II).

In Figs. 2 and 3 we presented the coagulation data obtained by Kim *et al.* [1] and by Rooker & Davies [2]. For comparison purposes, we have also included the simulation results that we obtained with the MFC model. In these fig-

ures we can observe that the MFC model was able to reproduce well the experimental data satisfactorily.

### 5. Turbulent brownian coagulation

In order to test the MFC model under turbulent conditions, we also tried to reproduce the experimental data obtained by Okuyama *et al.* [3]. The coagulation experiments in this case were carried out using an aerosol of tobacco smog particles. In these experiments, the aerosol was stirred with different speeds during 300 to 500 s (see Table IV), measuring the density of the number of tobacco particles at several times. Initial densities of the number of particles ranging from 1.30 to  $2.00 \times 10^7$  were used. For the computer simulations, we considered the experiments performed by Okuyama *et al.* [3] under low and medium turbulence intensity conditions (that is, with stirring speeds of 600, 1440 and 1800 rpm).

TABLE IV. General conditions of the turbulent coagulation experiments carried out by Okuyama *et al.* (1977)

| <b>Experimental conditions:</b>   |                     |          |                                     |  |  |
|---|---------------------|----------|-------------------------------------|--|--|
| - Aerosol: tobacco smog<br>- Constant temperature and pressure<br>- Stirring speeds: 600, 1440 and 1800 rpm<br>- Experiment duration: 300 – 500 s |                     |          |                                     |  |  |
| Stirring speed (rpm)  | $N_o$ ( $\#/cm^3$ ) | $\sigma$ | Mean geometric diameter ( $\mu m$ ) | Kinetic energy dissipation rate ( $\epsilon$ ), ( $cm^2/s^3$ ) |  |
| 600   | $2.00 \times 10^7$  | 1.34     | 0.94                                | 30,000   |  |
| 1440  | $1.30 \times 10^7$  | 1.34     | 0.94                                | 824,043  |  |
| 1800  | $2.00 \times 10^7$  | 1.31     | 0.84                                | 810,000  |  |

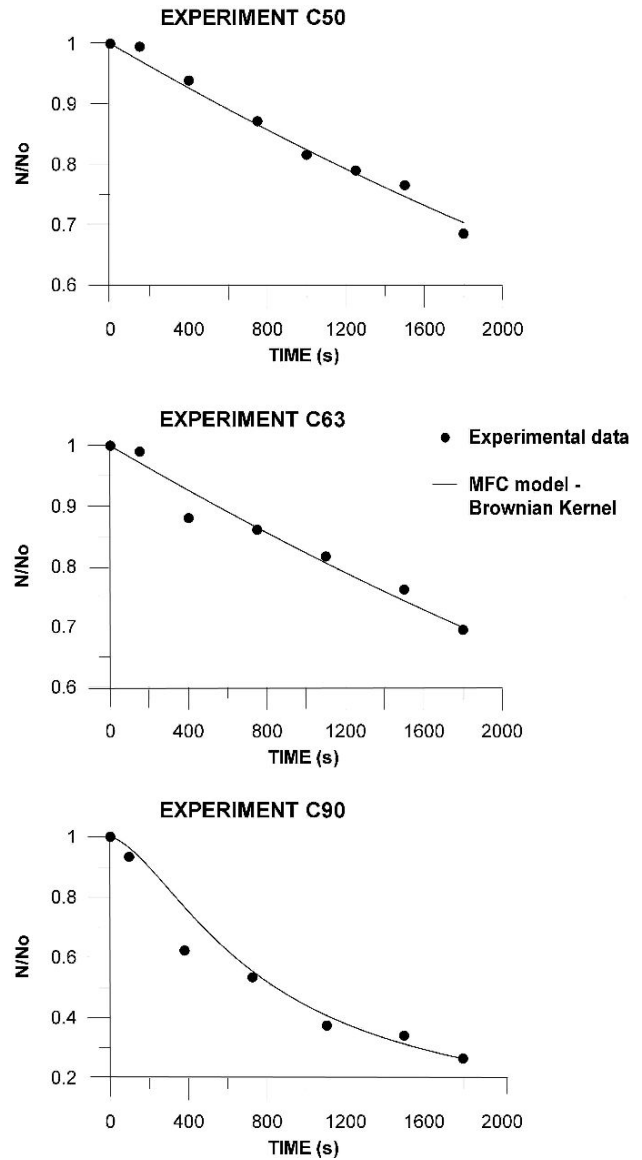
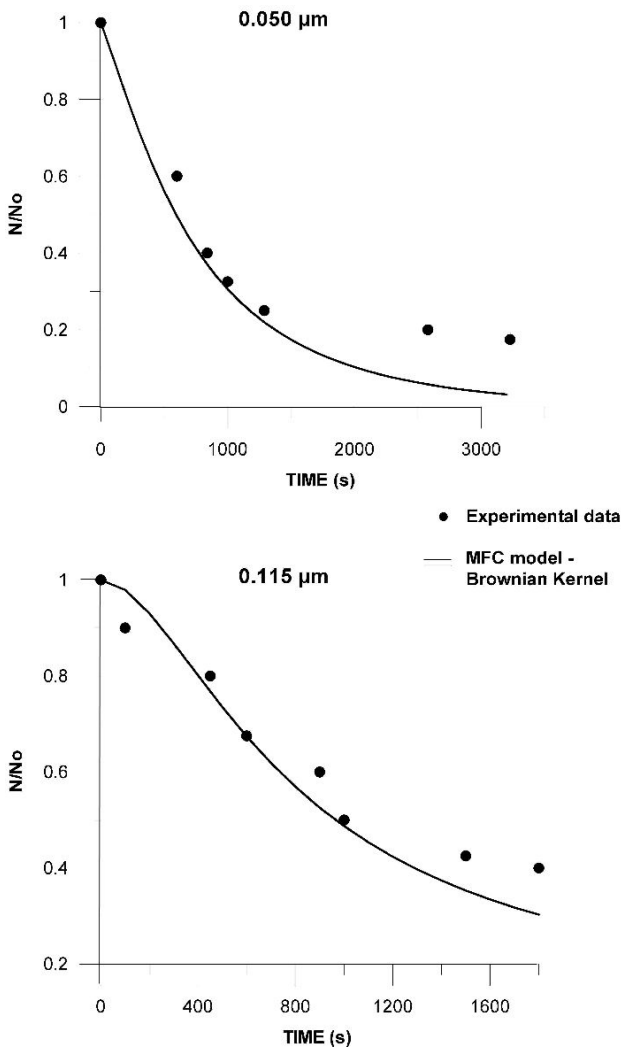


FIGURE 2. Brownian Coagulation. Comparison of the MFC model results (solid lines) for the density of the total number of aerosol particles as function of time against coagulation experimental data (circles) obtained by Kim *et al.* (2003) working with a NaCl aerosol.

FIGURE 3. Brownian Coagulation. Comparison of the MFC model results (solid lines) for the density of the total number of aerosol particles as function of time against coagulation experimental data (circles) obtained by Rooker & Davies (1979) using a  $CaCO_3$  aerosol.

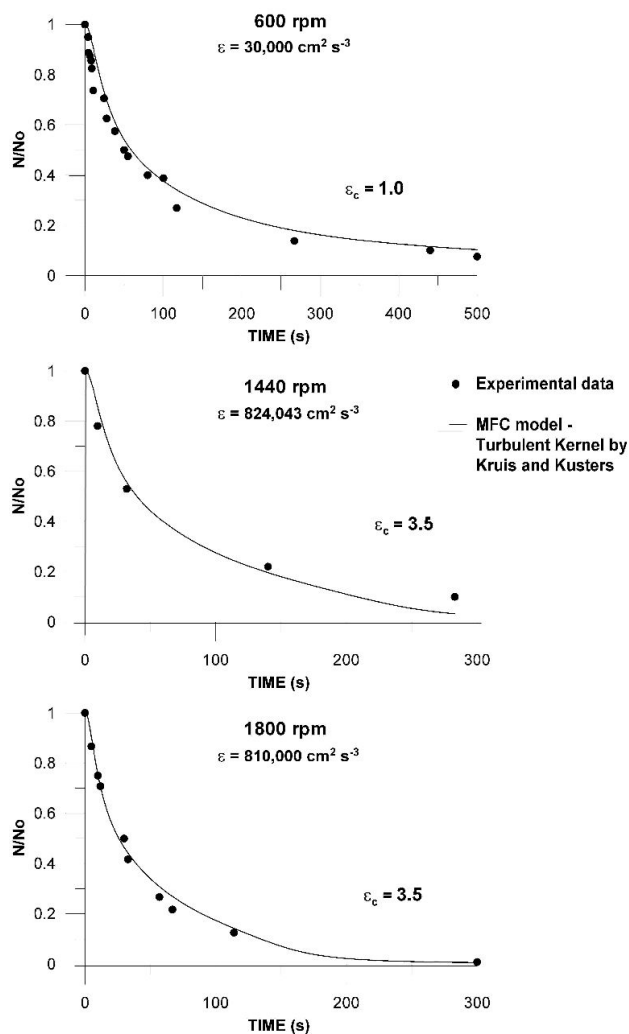


FIGURE 4. Turbulent Coagulation. Comparison of the estimates obtained with the MFC model against the turbulent coagulation experimental data obtained by Okuyama *et al.* (1977) working with a tobacco smog aerosol stirred at 600, 1440 and 1800 rpm.

In the simulations with the MFC model, it was considered a range of particle diameters from 0.08 to 5.50  $\mu\text{m}$ , which includes more than 90% of the particles which were present in each experiment. This range was divided in the following nine subintervals: 0.08 – 0.10, 0.10 – 0.20, 0.20 – 0.32, 0.32 – 0.64, 0.64 – 1.24, 1.24 – 2.00, 2.00 – 2.50, 2.50 – 4.00, and 4.00 – 5.50  $\mu\text{m}$ . The densities of the number of particles for each interval were numerically calculated in the simulations for times of 300 and 500 s, using a time step of 1 s. With these densities, it was calculated the density of the total number of particles also as function of time.

In Fig. 4 we presented the experimental data (circles) and the results obtained with the MFC model (solid lines) for the different stirring-speeds we considered. For the coagulation experiment carried out at low turbulence intensity (600 rpm) we used a collision efficiency  $\varepsilon_c = 1$ , and for the experiments performed at medium turbulence intensity (1440 and 1800 rpm) we used  $\varepsilon_c = 3.5$ . It can be observed in these figures that the MFC model also was able again to reproduce satisfactorily well the coagulation experimental-data of Okuyama *et al.* (1977).

## 6. Conclusions

In this paper, we presented a simple mean field coagulation model for polydispersed aerosols, as well as the results found using such a model to reproduce numerically data obtained by Kim *et al.* (2003) and Rooker & Davies (1979) in experiments of pure brownian coagulation, and by Okuyama *et al.* (1977) in experiments of turbulent brownian coagulation. No matter the simplicity and the mean field nature of the model, the simulations carried out showed a very satisfactory agreement between its estimates and the experimental data for the density of the total number of aerosol particles. It would have also be interesting to have compared the simulation results obtained for the number of densities at each subinterval of particle diameters, however, no experimental results were found in literature about this item.

1. D.S. Kim, S.H. Park, Y.M. Song, D.H. Kim, and K.W. Lee, *J. Aerosol Sci.* **34** (2003)859.
2. S.J. Rooker and C.N. Davies, *J. Aerosol Sci.* **10** (1979)139.
3. K. Okuyama, Y. Kousaka, Y. Kida, and T. Yoshida, *J. Chem. Eng. Japan.* **10** (1977)142.
4. S.K. Friedlander, *Smoke, Dust and Haze. Fundamentals of Aerosol Dynamics*, 2a. ed. (Oxford New York: Oxford University Press, 2000).
5. J.H. Seinfeld and S.N. Pandis, *Atmospheric Chemistry and Physics. From Air pollution to Climate Change*, 1a. ed. (John Wiley & Sons, Inc., E.U.A., 1998).
6. S.H. Park, F.E. Kruijs, K.W. Lee, and H. Fissan, *Aerosol Sci. and Technol.* **36** (2002) 419.
7. S.H. Park, F.E. Kruijs, K.W. Lee, and H. Fissan, *Evolution of Particle Size Distributions due to Turbulent and Brownian Coagulation* (2000) <http://www.uni-duisburg.de/FB9/AMT/reports/amtfgd2000.pdf>.
8. D. Pnueli, D. Gutfinger, M. Fichman, *Aerosol Sci. and Technol.* **14** (1991) 201.
9. M.M.R. Williams, *J. Phys. D: Appl. Phys.* **21** (1988) 875.
10. J.H. Seinfeld, *Atmospheric Chemistry and Physics of Air Pollution*, 1a. ed. (John Wiley & Sons, Inc., E.U.A., 1986).

11. F. Gelbard and J.H. Seinfeld, *J. Colloid Interface Sci.* **68** (1979) 363.
12. M. Molina (private communication 2004).
13. S. Suck and J.R. Brock, *J. Aerosol Sci.* **10** (1979) 581.
14. M.Z. Jacobson, R.P. Turco, E.J. Jensen, and O.B. Toon, *Atmos. Environ.* **28** (1994) 1327.
15. M.Z. Jacobson, *Fundamentals of Atmospheric Modeling*, 1a. ed. (Cambridge University Press, E.U.A., 1999).
16. M.Z. Jacobson, *J. Geoph. Res.* **108** (2003) AAC 4-1.
17. A. Prakash, A.P. Bapat, and M.R. Zachariah, *Aerosol Sci. and Technol.* **37** (2003) 892.
18. L.I. Zaichik and A.L. Solov'ev, *High Temperature* **40** (2002) 422.
19. P.G. Saffman and J.S. Turner, *J. Fluid Mech.* **1** (1956) 16.
20. J. Abrahamson, *Chem. Eng. Sci.* **30** (1975) 1371.
21. F.E. Kruis and K.A. Kusters, *Chem. Eng. Comm.* **158** (1997) 201.